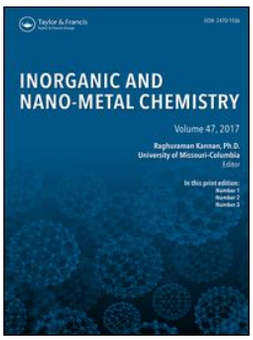

Taylor & Francis
Taylor & Francis Group

Inorganic and Nano-Metal Chemistry

ISSN: (Print) (Online) Journal homepage: https://www.tandfonline.com/loi/lsrt21

Study of biogenically fabricated transition metal oxides nanoparticles on oral cavity infectious microbial strains

Madiha Batool , Shazia Khurshid , Zahid Qureshi , Ali Hassan , Muhammad Bilal Ahmed Siddique , Sabiha Naveed & Sabir Ali Siddique

To cite this article: Madiha Batool , Shazia Khurshid , Zahid Qureshi , Ali Hassan , Muhammad Bilal Ahmed Siddique , Sabiha Naveed & Sabir Ali Siddique (2020): Study of biogenically fabricated transition metal oxides nanoparticles on oral cavity infectious microbial strains, Inorganic and Nano-Metal Chemistry, DOI: 10.1080/24701556.2020.1811729

To link to this article: https://doi.org/10.1080/24701556.2020.1811729

Published online: 31 Aug 2020.

INORGANIC AND NANO-METAL CHEMISTRY
https://doi.org/10.1080/24701556.2020.1811729

Study of biogenically fabricated transition metal oxides nanoparticles on oral cavity infectious microbial strains

Madiha Batool[a], Shazia Khurshid[a], Zahid Qureshi[a], Ali Hassan[a], Muhammad Bilal Ahmed Siddique[b], Sabiha Naveed[c], and Sabir Ali Siddique[c]

[a]Department of Chemistry, Government College University, Lahore, Pakistan; [b]Department of Chemistry, Government College University, Faisalabad, Pakistan; [c]Institute of Chemistry, University of the Punjab, Lahore, Pakistan

ABSTRACT

The selected six specific bacterial and fungal strains, which caused oral teeth decay were analyzed by antimicrobial iron oxide (Fe_2O_3), copper oxide (Cu_4O_3), and zinc oxide (ZnO) nanoparticles synthesized by *aloe barbadensis* leaves extract, using agar well diffusion method with 0.9% saline solution. TMOs comparatively had not been focused on oral cavity infectious pathogens to analyze antimicrobial activity. In the present study, TMOs were characterized by UV, SEM, FTIR, and XRD. Oral infectious strains (*Escherichia coli, Bacillus subtilis, Bacillus licheniformis, Klebsiella pneumonia)* and fungal strains (*Aspergillus niger*, *Candida albicans*) were used as test microorganisms. The effect of different concentrations of TMO-NPs (2.5 μg/mL, 5 μg/mL, 10 μg/mL) was studied by zone of inhibition (ZOI), minimum inhibitory concentration (MIC), and minimum bactericidal concentration (MBC). The zinc oxide nanoparticle with least particle-sized (37.8 nm) exhibited highest antimicrobial activity. In future, these zinc-oxide nanoparticles may be used in medicine for oral infectious diseases treatment.

ARTICLE HISTORY
Received 2 May 2020
Accepted 26 July 2020

KEYWORDS
Nanomaterial; X-ray diffraction (XRD); antibacterial activity; metal oxides; antifungal activity

Introduction

Nanotechnology has attained a great deal of attention in the scientific circle. Nanomaterials like copper, zinc, and iron oxides had been used in industry for different purposes, like paints, cosmetics, and plastics. Transition metal oxides had strong antibacterial activity.[1–3] The development of efficient green chemistry methods for transition nano metal oxides fabrication had been investigated to find an eco-friendly technique for production of well-characterized nanoparticles as in Table 1. This study aims at the role of the biological component, essential phytochemicals (e.g., alkaloids, terpenoids, amides, and aldehydes) as reducing agent and solvent system.[4,5]

Aloe barbadensis Miller (Aloe Vera) belong to Aloeaceae family, genus *Aloe vera* in which Barbadensis Miller, Aborescens, and Chinensis are familiar.[6,7] Additionally, Aloe vera plant leaves extract contains a viscous substance which carries vitamins A, C, antioxidants like beta-carotene, choline, folic acid, and also contains antioxidants like calcium, copper, magnesium, potassium, and zinc, necessary for the functioning of an enzyme in many metabolic pathways.[8–13] Aloe vera gel is used in food flavoring, cosmetics, food supplement and herbal remedies, which is enriched in cholesterol, campesterol, steroids, sitosterol, and lupeol having an anti-inflammatory property, it is also comprised of salicylic acid an anti-inflammatory agent, carboxymethyl, and sulphoxy groups.[14] These chemicals in a plant like salicylic acid and anthraquinones (aloin, aloetic acid, anthranol, cinnamic acid, and anthracene) are responsible for the one-step reduction of metals in biogenic synthesis.[15,16] Polyphenols (aloin) in aloe vera leaves extract can act as a chelating agent, capping and reducing agents for the biogenic formulation of metal nanoparticles.[17] The researchers also compared the germ-killing ability of *Aloe barbadensis* in tooth gums in cavities. They realized that the aloe vera gel was as better than the commercial kinds of toothpaste at fighting cavity-causing oral infectious bacteria.[18] The *Aloe barbadensis* gel contains compound anthraquinones that heal and recover pain by natural anti-inflammatory effects. *Aloe barbadensis* had also beneficial effects on human health. The scientists discovered their antimicrobial and antimycoplasmic activities. Antimycoplasmic substances present in plant help in the destruction of bacterial strains.[19]

The nano-sized metal oxides had modified physical, morphological, optical, and chemical properties. The antimicrobial activity deals with inhibiting disease-causing microbes. Owing to adventure in the nano-biotechnology field, nano metal oxides of desired size and shape, lead to the buildout of antibacterial agents. Many antimicrobial agents were used for this purpose with different modes of action. Nano metals oxides play a vital role as an antimicrobial agent.[13,20–22] The mechanism of microbial activity of MO-NPs was analyzed by membrane damage, metal ion homeostasis disturbance, and enzymes dysfunctioning. MO-NPs exhibit anti

CONTACT Madiha Batoola tweetchem56@gmail.com Department of Chemistry, Government College University, Lahore, Pakistan; Sabir Ali Siddiquec sabir.siddique@hotmail.com; sabirali2014@gmail.com Institute of Chemistry, University of the Punjab, Lahore, Pakistan.

Table 1. Plant species responsible for MO-NPs.

Plant species	MO-NPs	Active component	Size	Antimicrobial applications
Glycosmis Mauritania	Fe_3O_4	Triterpenes, eugenol	58–79 nm, spherical	*E. coli*
Cassia Fistula	ZnO	Polyphenols, flavonoid	5–15 nm hexagonal	*P. aeruginosa*
Phyllanthus Amarus	CuO	Not mention	50 nm	*S. aureus*
Aloe Barbadensis	ZnO	Flavanones, terpenoids	25–40 nm spherical	*M. luteus*
Sageretia thea	Fe_2O_3	Polyols	Below 100 nm	*B. cereus*
Parthenium hysterophorus	ZnO	Proteins	27–84 nm hexagonal	*S. typhimurium*
Ocimum basilicum	ZnO	Flavanones,terpenoids	50 nm hexagonal	*S. enteritidis*
Solanum lycopersicum	ZnO	Not mention	25 nm hexagonal	*K. pneumoniae*
Camellia sinensis	Fe_2O_3	Carboxyl, hydroxyl, amine groups and proteins	60 nm mesoporous	*P. aeruginosa*
Sapindus mukorossi	Fe_2O_3	Flavonoids	Below 100 nm	*K. pneumoniae*
Hibiscus rosa-sinensis	Cu_4O_3	Phenolic compound	30–50 nm	*E. coli*
Aloe barbadensis	Fe_2O_3	Proteins, terpenoids	20–60 nm	*S. aureus*
Aloe barbadensis	CuO	Carbonyl groups	15–30 nm versatile	*S. epidermidis*
Eucalyptus globulus	Fe_2O_3	Phenols and proteins	Below 100 nm	*E. faecalis*
gum karaya	CuO	Carbohydrates, proteins	7.8 nm irregular	
Hibiscus subdariffa	ZnO	carboxylic acids, phenol	20–45 nm hexagonal	*B. cepacia*
Padina pavonica	Fe_3O_4	Not mention	19.5–27 nm	*E. coli*
Calotropis Procera	ZnO	amine groups , proteins	5–40 nm. spherical , granular	*P. fluorescens*
Arachis hypogaea	Cu_2O	Phenolic compound	37 nm	*S. putrifaciens*
Azadirachta indica	Cu_4O_3	Flavanones or terpenoids	~28–30 nm tetragonal	*S. maltophillia*
Aloe barbadensis	Cu_4O_3	Phenols and proteins	30–60 nm	*K. pneumoniae*

Table 2. Mechanism of antibacterial activity of by Nanomaterial.

Sr.No	Nanomaterial	Mechanism of antibacterial activity	MIC reduction	Bacteria
1	ZnO	ROS inhibition	95%	*S. aureus*
2	TiO	Cell membranes damage	50%	*E. coli*
3	Ag	Cell wall disruption	100%	*E. coli*
4	CuO	Protein inactivation	90%	*B. subtilis*
5	Fe_3O_4	ROS disruption	65%	*S. aureus*
6	Al_2O_3	Flocculation, ROS	57%	*B. subtilis*

bactericidal properties by the generation of reactive oxygen species which are capable to target metabolic pathways by reducing DNA synthesis of prokaryotic cells leading to cell death.[2,5,7] The gram-positive (GP) and gram-negative (GN) bacterial strains create a severe health problem. Increased infection of pathogenic strains may cause new bacterial mutations, lack of vaccine, and health hazards. The different infectious diseases caused by test organisms in present research could be analyzed in Table 2. The bacterial cell wall is composed of peptidoglycan. The metal oxides nanoparticles can pass through the bacterial cell wall and susceptible to destruction. The precise mechanism of antimicrobial activity by TMO-NPs is under consideration, although it may be due to binding with DNA cytosolic and protein of pathogens, metabolic pathways adenosine triphosphate (ATP) production and respiratory dysfunctioning.[23] Antibacterial and antifungal activity of metal oxide nanoparticles depends on the size, stability in the environment, and concentration in the medium growth.[24] As metal oxide nanoparticles had small in size than bacterial pores they could cross the cell membrane of pathogenic bacteria and fungi.[25] Transition metals oxides possess the catalytic and photochemical activity and are beneficial in antimicrobial response. Our work was intended to explore further investigation of new techniques from transition metal oxides unique features. Oral hygiene referred to dental trauma, cavity and gingivitis problems caused by metabolization of carbohydrates to organic acids. Dental infectious diseases caused by infectious pathogens imposed financially burden as seen in Table 3. Oral hygiene is considered important for avoiding tartar to prevent tooth decay and periodontal diseases. Owing to adverse actions of chemical treatments transition nano metal oxides emerged out as the best remedy. Metal oxide nanoparticles had been used in research as treatment of infectious diseases caused by pathogenic bacterial and fungal strains. This research was intended to explore the antibacterial and antifungal activity of biogenically synthesized transition metal oxides. The novelty of work is a unique comparison of biogenically fabricated three transition metal oxides and their comparative study of antimicrobial activity against oral cavity infectious microbial strains.

Materials and methods

Synthesis of Aloe barbadensis leaves extract

Aloe barbadensis plant was purchased from the botanical garden of GCU Lahore. The leaves extract was prepared by washing 25 g leaves with distilled water. The obtained leaves material were dissolved in 100 mL of water in a 250 mL flask and allowed to boil for 30 min at 80 °C and then allowed to cool down at room temperature. The resulting solution was filtered twice using a 0.2-micrometre filter paper to remove any impure particles.

Fabrication of nano transition metal oxides

Fifty milliliters solution of 0.4 M, 0.5 M, and 0.2 M solutions of salts 99% purity technical grade copper sulfate ($CuSO_4$), 98% pure ferric chloride ($FeCl_3$), 99% pure zinc nitrate ($ZnNO_3$) was added respectively into 25 mL Aloe vera leaves extract in a 250 mL Erlenmeyer flask with constant shaking with a magnetic stirrer under heating at temperature 100–120 °C range. Then the resultant solution underwent centrifugation by using (Beckman JA-17 rotor model), at 10,000 rpm for 10–15 min, at temperature 35 °C and solid particles were collected after discarding the supernatant. The particles were washed twice with

Table 3. Infectious diseases caused by bacterial strains.

Strains	Identification	Infections in human
Escherichia coli	Gram negative bacteria	Cholecystitis, cholangitis, bacteremia, Diarrhea, UTI
Bacillus subtilis	Gram positive bacteria	Infection in the respiratory tract, eye, ears urinary tract
Bacillus licheniformis	Gram-positive bacteria	Septicemia, endocarditis, bacteremia, diarrhoeal illness
Klebsiella pneumonia	Gram negative bacteria	Liver abscess,pneumonia,septicemia,nosocomial infections

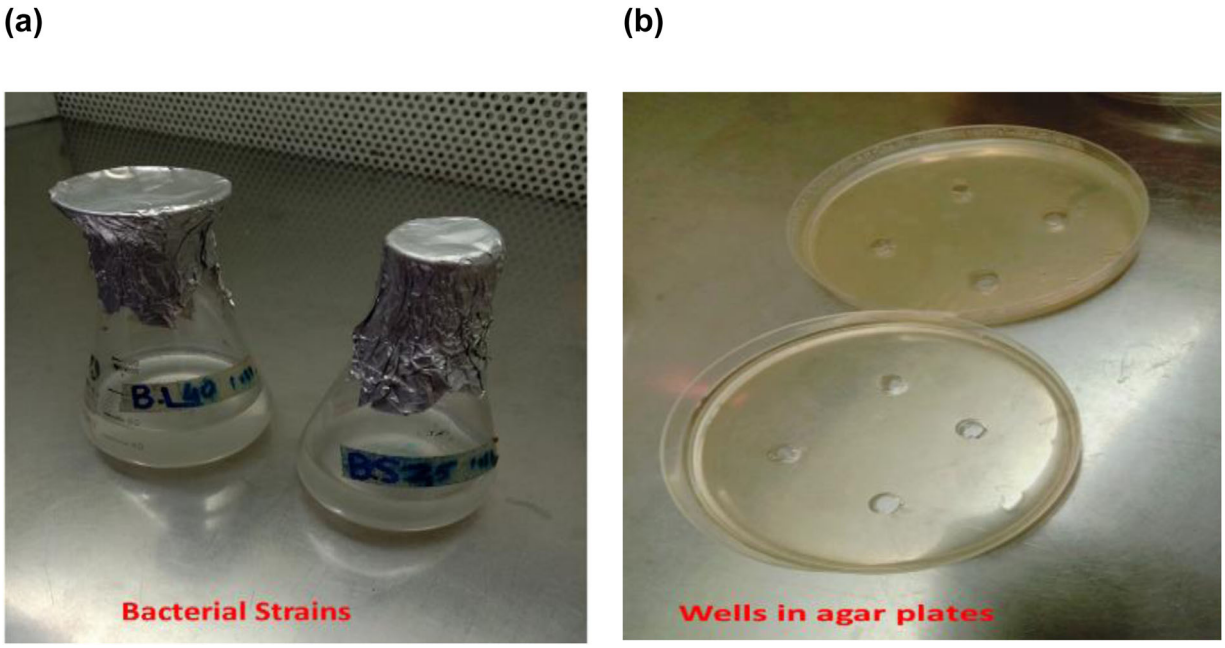

Figure 1. (a) Bacterial strain growth (b) Punching of wells in agar plates.

deionized water and ethanol. The collected MO-NPs were dried in a watch glass for evaporation of extra liquid. The formed precipitates were annealed at 500 °C for 2 h followed by grinding for further characterization.

Characterization of transition metal oxides nanoparticles

Morphology of transition metals oxides was using scanning electron microscopy (SEM). X-ray diffraction patterns were obtained with copper radiation by using diffractometer. The correct calculations were made by step scanning program and analyzed by X-pert high score software. The crystalline size was calculated by the Scherrer equation. Fourier transform infrared spectroscopy (FTIR) spectra were analyzed in the 400−4000 cm^{-1} spectral region. The nanometals oxides powders were palletized with potassium bromide (KBr) for results. Ultraviolet (UV) spectra of three metal oxides were monitored as time function by spectrophotometer in 200–800 nm range at a resolution of 1 nm.

Antimicrobial activity

Bacterial and fungal strains

Bacterial strains: *Escherichia coli, Bacillus subtilis, Bacillus licheniformis, Klebsiella pneumonia*

Fungal strains: *Aspergillus niger, Candida albicans*

Preparation of microbial inoculum

Bacterial and fungal test organism strains were grown in nutrient agar for about 24 h at 37 °C. The 0.9% saline solution was prepared in the 100 mL flask and autoclaved to remove contamination. The test microorganism was inoculated in the saline solution with the help of the inoculating loop. A loop full of 24 h old culture was taken and inoculated in the pre autoclaved 0.9% saline solution. The turbidity of the cultures was adjusted with 0.5 Mcfarland. This flask was placed in the incubator shaker to properly mix the microorganism. For MIC calculation, the nutrient broth was prepared in 100 mL flask and was autoclaved. The nutrient broth was inoculated for 24 h and hold fresh culture with the help of the inoculating loop. The nutrient broth was placed in an incubator shaker at 37 ± 0.5 °C, speed of 170 rpm for 24 h.

Agar well-diffusion method

To evaluate antimicrobial activity, agar well diffusion method was applied in which the surface of agar plates was inoculated by microbial inoculum volume over agar surface. Conical flask of 100 mL of nutrient broth was incubated overnight with tested microorganisms at 37 °C. During incubated on nutrient agar at 35 °C about 18 h, we suspended a 0.9% saline solution. With sterile pipette application about 0.6 mL of broth mixed in 60 mL of molten agar and poured into a petri dish to cool. Agar plates with 0.3 mL of all bacterial and fungal strains were prepared and allowed to set. Four wells of about 5 mm diameters were punched and sealed with a sterile cork borer (Figure 1). In one hole bacterial and fungal strains were loaded while in the other three holes 100 µg/mL TMO-NPs sample with a concentration of

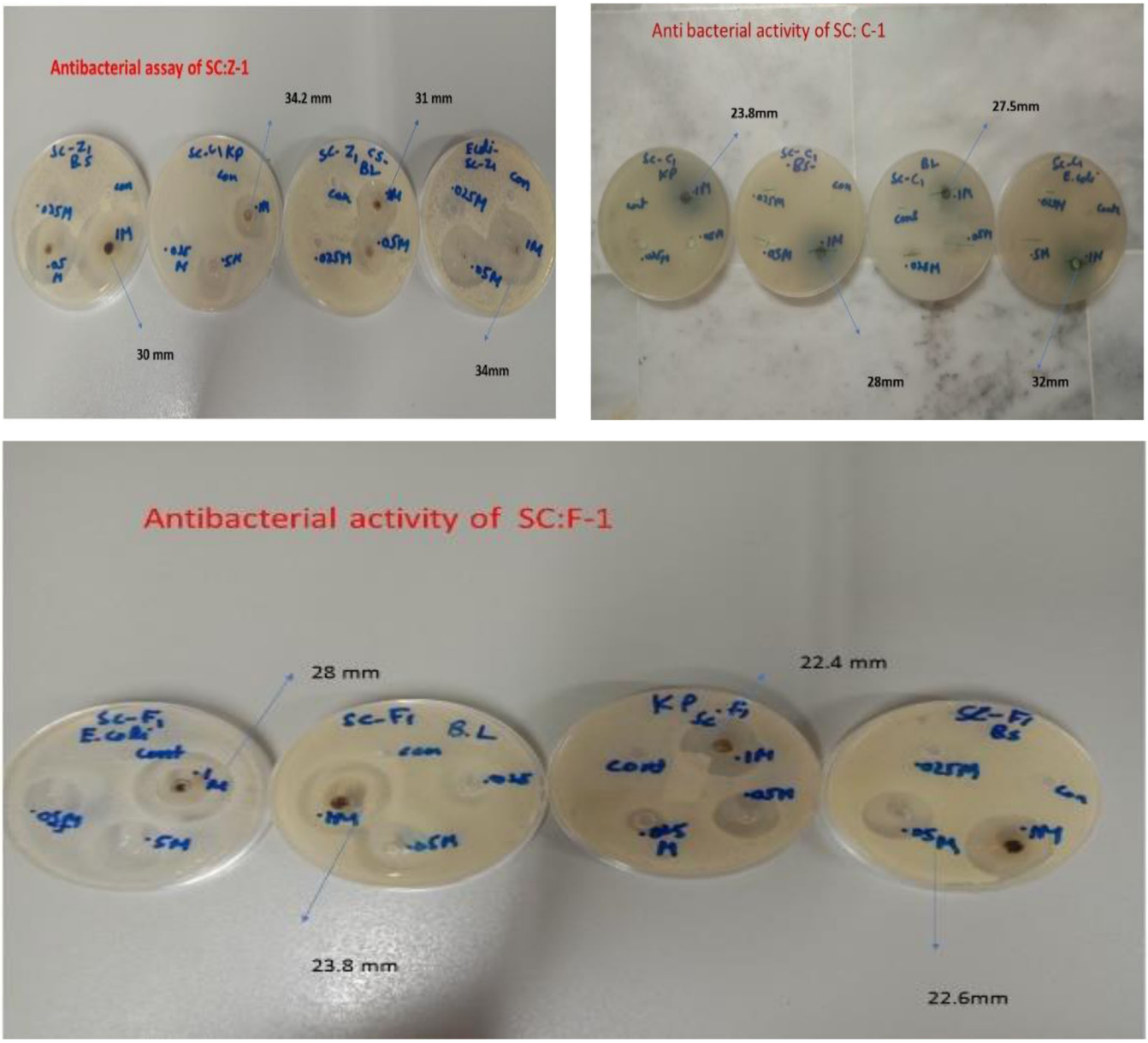

Figure 2. Antibacterial assay of sample code SC:,Z-1,F- 1 and C-1 against *Escherichia coli*, *Bacillus subtilis*, *Bacillus licheniformis*, *Klebsiella pneumonia* bacterial strains.

Table 4. Antimicrobial activity of zinc oxide nanoparticles (ZOI, MIC, and MBC) as biogenically fabricated against laboratory bacterial and fungal strains by using the maximum concentration of 10 µg/ml.

Bacterial strains	ZOI mm	ZOI mm (24 h)	MIC (µg/mL)	MBC (µg/mL)	Control Negative
Escherichia coli	34	37	1	0.8	null
Bacillus subtilis	30	33	1.2	1	
Bacillus licheniformis	31	34	1.2	1	
Klebsiella pneumonia	34.2	36.2	1.3	1.1	
Aspergillus niger	17.5	20.5	1.7	1.2	
Candida albicans	16.1	19.6	2	1.4	

Table 5. Antimicrobial activity of iron-oxide nanoparticles (ZOI, MIC, and MBC) as biogenically fabricated against laboratory bacterial and fungal strains by using the maximum concentration of 10 µg/ml.

Bacterial strains	ZOI mm	ZOI mm (24 h)	MIC (µg/mL)	MBC (µg/mL)	Control Negative
Escherichia coli	28	30.4	2.5	2.3	null
Bacillus subtilis	22.6	24.5	4.4	4.1	
Bacillus licheniformis	23.8	26.5	4.3	3.7	
Klebsiella pneumonia	22.4	22.9	4.5	4.1	
Aspergillus niger	9.4	11.7	5	4.6	
Candida albicans	9.1	12.1	4.7	4.2	

2.5 µg/ml, 5 µg/ml, and 10 µg/mL was loaded. The plates were left for two hours at room temperature and then overnight at 37 °C. Zone of inhibition (ZOI) was calculated by measuring growth with scale. An experiment was conducted thrice to calculate concordant readings. The Petri plates used for antibacterial activity after calculation size of the ZOI are shown in Figure 2.

MIC and MBC determination

The broth dilution assay was conducted to calculate the minimum inhibitory concentration (MIC) and minimal bactericidal concentration (MBC).

MIC determination

Minimum inhibitory concentration is the lowest nano metal oxides amount which inhibited the microorganism growth. MIC was determined by solution preparation of MO-NPs in different concentrations, incubation with microbial strains and results calculation by broth microdilution. Three main reagents were media (Hinton broth; support growth of pathogen), tested microbe (bacterial and fungal strain), and antimicrobial agents (MO-NPs). The concentration of antimicrobial agents was adjusted with media. To obtain serial dilution of concentration (0.5–10 µg/mL) prepared to obtain gradient. By adjusting incubation time and dilution bacterial and fungal strains added, inoculated tube and incubated for 20 h. MIC was finally calculated by turbidity level.

MBC determination

Minimum bacterial concentration is the lowest MO-NPs concentration killing maximum bacteria inoculum with no visible growth. MBC was determined by subculturing of tubes which had no growth on the agar plate. Almost 200 µL of tubes content without turbidity were cultured on Muller Hinton agar media and incubated for 24 h and examined for growth. The tube which has the lowest MO-NPs concentration and fails to grow on culture was MBC of test microbial strain, MIC and MBC results were summarized in Tables 4–6.

Table 6. Antimicrobial activity of copper oxide nanoparticles (ZOI, MIC, and MBC) as biogenically fabricated against laboratory bacterial and fungal strains by using the maximum concentration of 10 µg/ml.

Bacterial strains	ZOI mm	ZOI mm (24 h)	MIC (µg/mL)	MBC (µg/mL)	Control Negative
Escherichia coli	32	34.6	2.6	2.4	null
Bacillus subtilis	28	29.7	2.9	2.8	
Bacillus licheniformis	27.5	29	3.1	Np	
Klebsiella pneumonia	23.8	25.8	2.9	2.7	
Aspergillus niger	12	15.2	4.3	4	
Candida albicans	11.5	14.5	4.1	3.7	

Results and discussion

Characterization results

The maximum absorption peak was noted between the ranges of 200 and 250 nm for copper oxide nanoparticles. The peak of nanoparticles in this study appeared at about 230 nm with the maximum absorbance of 4, which confirmed the formation of copper oxide nanoparticles. The intense peak at about 230 nm was due to the interband transition of the core electrons of the sample. The sizes of the copper oxide nanoparticles were analyzed by using FWHM data in Debye Scherrer equation. The average particles size was analyzed between 20 and 40 nm. The Fourier transform infrared spectra of the SC: C-1(AV) was determined for functional group analysis. The bands at different positions correspond to stretching and bending of the functional group present. The different peaks were observed between the ranges of 400 and 4000 cm^{-1}. The broad bands were observed at 3230–3270 cm^{-1} correspond to the hydroxyl (OH) functional group stretching due to the presence of

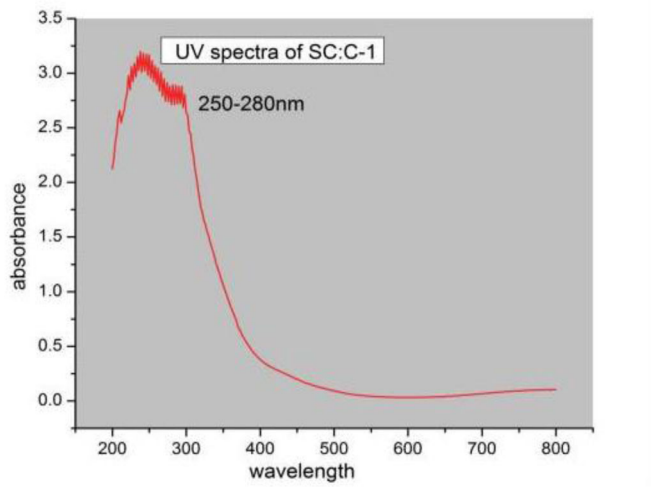

Figure 4. UV analysis of copper oxide (CuO) biogenically fabricated nanoparticles.

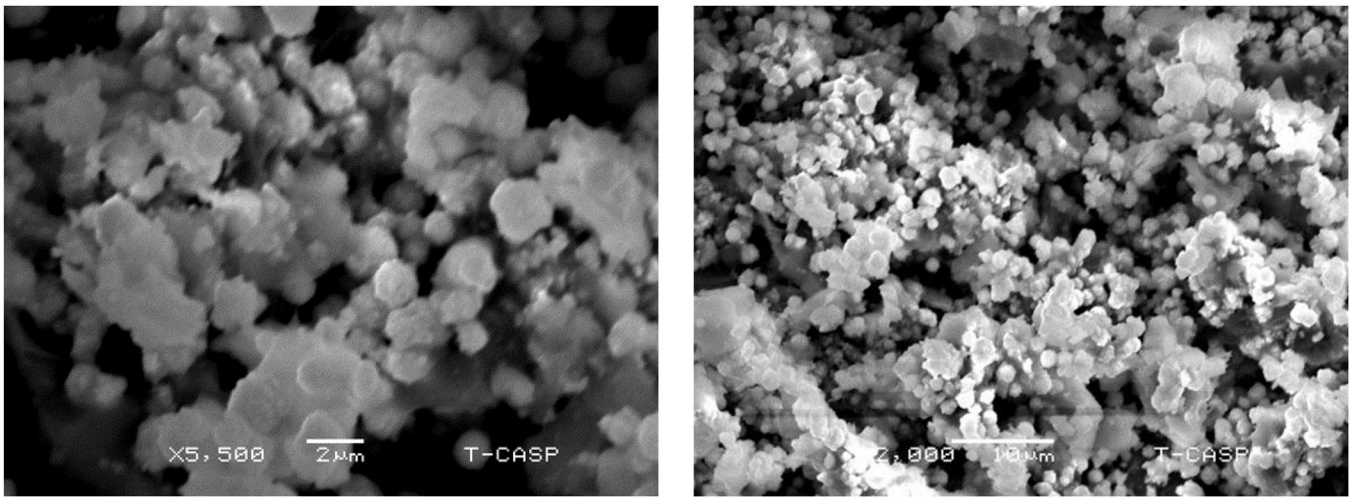

Figure 3. SEM analysis of copper oxide (CuO) biogenically fabricated nanoparticles.

alcohols and phenolic compounds of extract. The peaks between a range of 2930–2925 cm^{-1} and 1605–1615 cm^{-1} indicated the C–H and amide –NH group stretching,

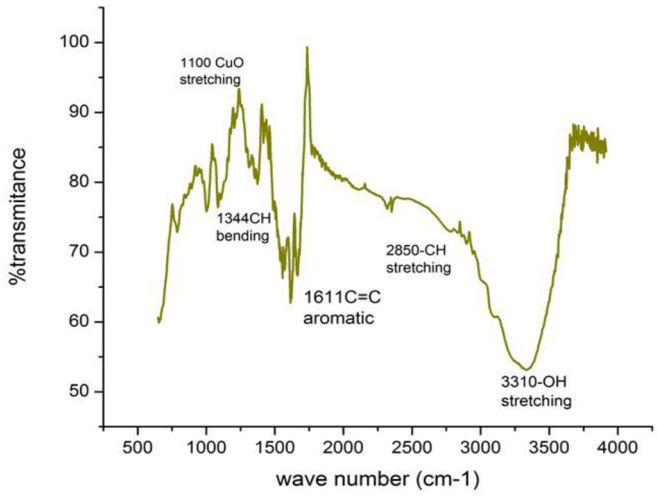

Figure 5. FTIR analysis of copper oxide (CuO) biogenically fabricated nanoparticles.

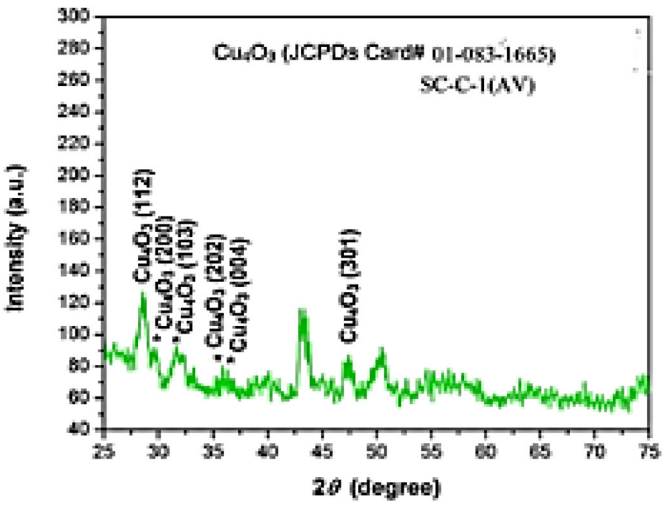

Figure 6. X-ray diffraction (XRD) analysis of copper oxide (CuO) biogenically fabricated nanoparticles.

respectively. According to the results shown in Figures 3–6, the analysis of copper oxide nanoparticles exhibited mostly tetragonal and a little bit irregular shape morphology with a smooth surface under the Scanning Electron Microscopy.

The reduction of zinc metal ion was monitored by aliquots subsequently checked by ultraviolet spectrophotometer at a range of 200–1100 nm and observed the peak of zinc oxide nanoparticles between 200 and 280 nm region. The average crystallite size was calculated at about 37.86 nm by XRD sheerer equation. The Fourier transform infrared (FTIR) spectra of the SC: Z-1(AV) biogenically fabricated by aloe barbadensis leaves extract determined between ranges of instrument 500–4500 cm^{-1} for functional group analysis. Notably, the functional group played an important role in ZnO-NPs synthesis. The broad bands observed at 3300–3470 cm^{-1} correspond to the alcoholic hydroxyl (OH) functional group stretching of precursor extract. The peaks between a range of 2920–2950 cm^{-1} and 1605–1655 cm^{-1} confirmed the C–H bonding of amide –NH group stretching, respectively. For semi electron microscopy (SEM) analysis at different magnifications confirmed the formulation of zinc oxide NPs (Figures 7–10). Moreover, on the further substantiation of the zinc oxide nanoparticles exhibited a hexagonal shape with a smooth surface. From the picture, it was confirmed, the average size between 30 and 40 nm, which was in best agreement calculated by X-ray diffraction analysis (37.8 nm).

The absorbance was recorded in the visible range set between 200 and 400 nm and operated at ambient temperature, the peak appearance at 298 nm confirmed the formation of iron oxide nanoparticles. The particle size was calculated by Scherrer equation where β-diffraction peak broadening at full width and max intensity FWHM was calculated 0.85. The average crystallite size was calculated at about 36.33 nm. The peak at 3328 cm^{-1} exhibited OH group stretching of phenols, polyphenol, carbohydrates monomers (mannose), and proteins. The stretching peak at 2923 cm^{-1} suggested for asymmetrical and symmetrical CH– and CH_2– groups. The carbonyl group CO stretching of COOH group

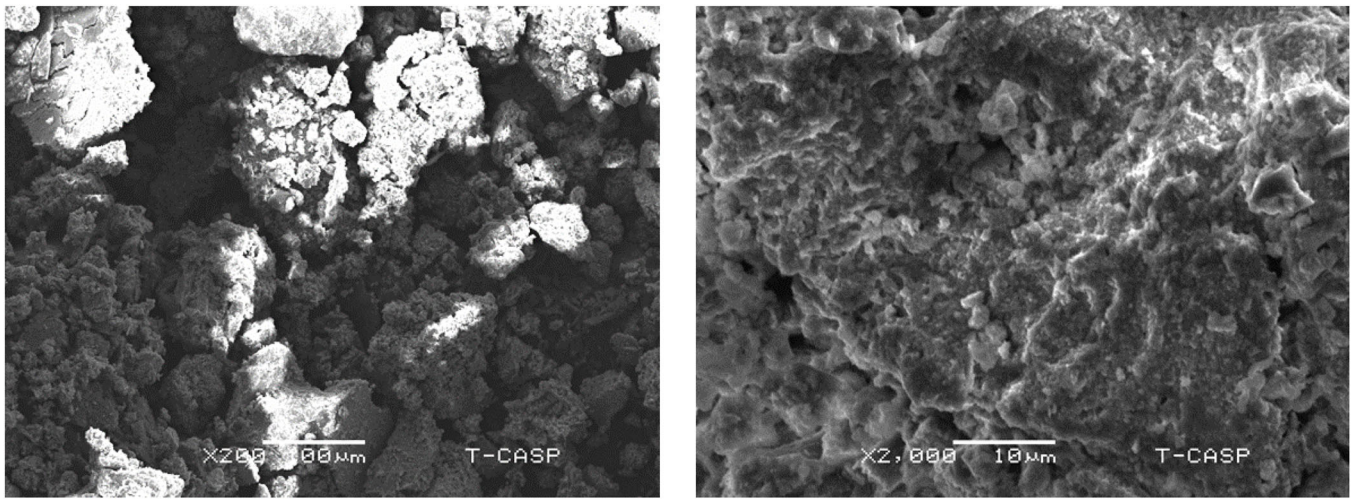

Figure 7. SEM analysis of zinc oxide (ZnO) nanoparticles.

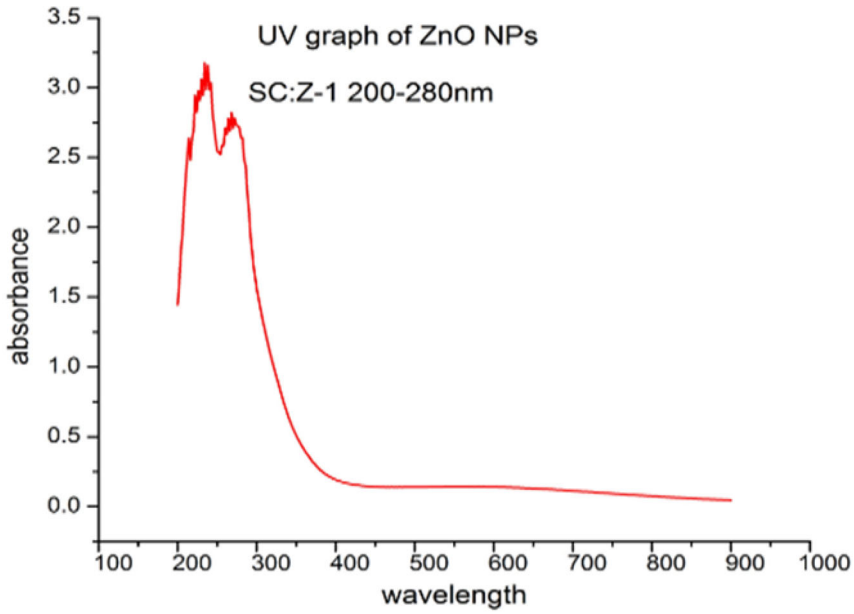

Figure 8. UV spectral analysis of zinc oxide (ZnO) nanoparticles.

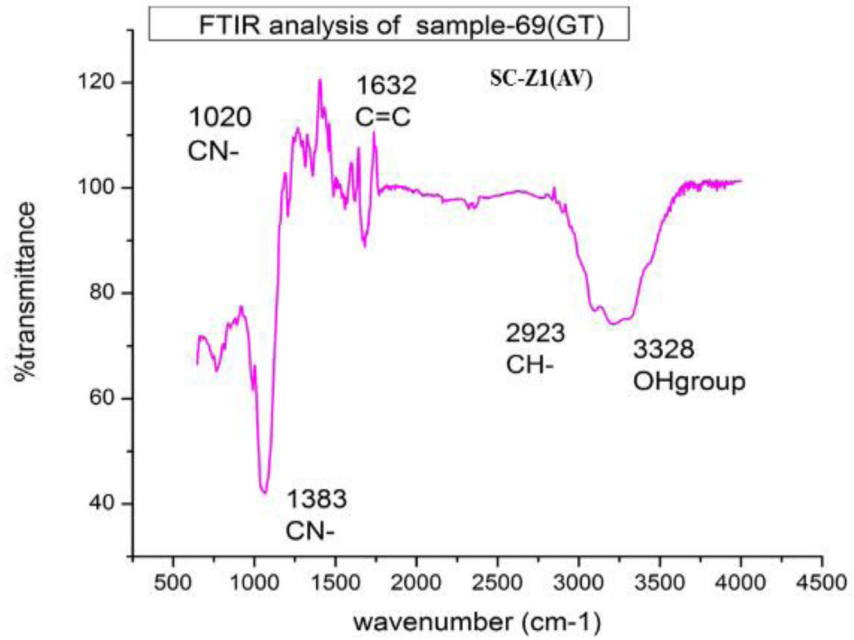

Figure 9. FTIR analysis of zinc oxide (ZnO) nanoparticles.

was examined at 1300 nm. The peaks at 1632 cm^{-1} and 1410 cm^{-1} were assigned to pectin in sample characteristic of esters and carboxylic COO– stretching. The weak peaks at 850–1000 cm^{-1} were due to CO– stretching associated with the pectin constituent galacturonan. The carbohydrate out of plane deformation was observed between regions 680–715 cm^{-1}. The strong peak at 580 cm^{-1} regions indicated the Fe–O stretching confirmed the iron oxide nanoparticles fabrication. The average grain size of iron oxide nanoparticles was between the ranges of 20–39 nm. The shape of SC: F-1(AV) was rhombohedral to pyramidal with a smooth surface. Results of characterization studies are summarized in Figures 11–14.

Antimicrobial tests

Results of antifungal and antibacterial activity revealed that ZnO and Cu_4O_3 nanoparticles have excellent potential for pathogenic bacterial strains and fungi as compared to iron oxide nanoparticles. It was examined that zinc oxide nanoparticles had the least particle size and surface/volume ratio as compared to copper oxide and iron oxide, due to which they exhibited efficient antimicrobial activity. For Iron oxide nanoparticles, ZOI values analyzed by assay were 28 mm, 22.6 mm, 23.8 mm, 22.4 mm, 9.4 mm, and 9.1 mm against microbial strains. Similarly, Zinc oxide nanoparticles ZOI values calculated were 34 mm, 30 mm, 31 mm, 34.2 mm,

17.5 mm, 16.1 mm and copper oxide ZOI against *E. coli, K. pneumonia* (gram-negative bacteria) *B. subtilis, B. licheniformis* (gram-positive bacteria) *A. niger, C. albicans* (fungal strains) were 32 mm, 23.8 mm, 27.5 mm, 28 mm, 12 mm, and 11.5 mm, respectively (Figure 2). After 24 h, it was analyzed that the ZOI values increased due to again bacterial growth. The ZOI values calculated after 24 h for zinc oxide nanometal were 37 mm, 36.2 mm, 33 mm, 34 mm, 20.5 mm, and 19.6 mm for *E. coli, K. pneumonia* (gram negative bacteria) *B. subtilis, B. licheniformis* (gram-positive bacteria) *A. niger, C. albicans* (fungal strains) (Figure 15).

The results of transition metal oxides ZOI values summarized in Tables 4–6. The ZOI by transition metal oxides against microbial strains showed that all have the efficient antimicrobial and antifungal ability. The samples code SC: Z-1 least sized exhibited highest (37 mm) ZOI inhibition against *E. coli* bacterial strain, while, SC:C-1 and SC: F-1 calculated maximum ZOI of 34.6 mm and 30.4 mm respectively against *E. coli* bacterial strain. Among the bacterial strains, *E. coli* examined maximum ZOI values with transition metal oxides in comparison to other bacterial strains inaugurated to be the least. Similar observations were found in the case of *B. subtilis, B. licheniformis* and *K. pneumonia*, where the ZOI exhibited by TMO-NPs (Fe_2O_3, Zn O, Cu_4O_3) were

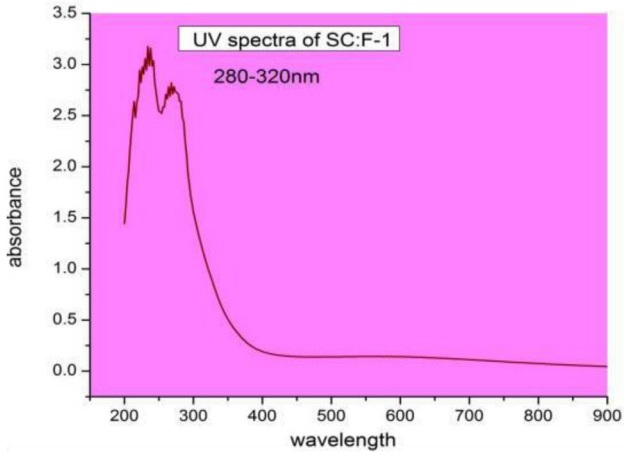

Figure 12. UV spectral graph of iron oxide (Fe_2O_3) biogenically fabricated.

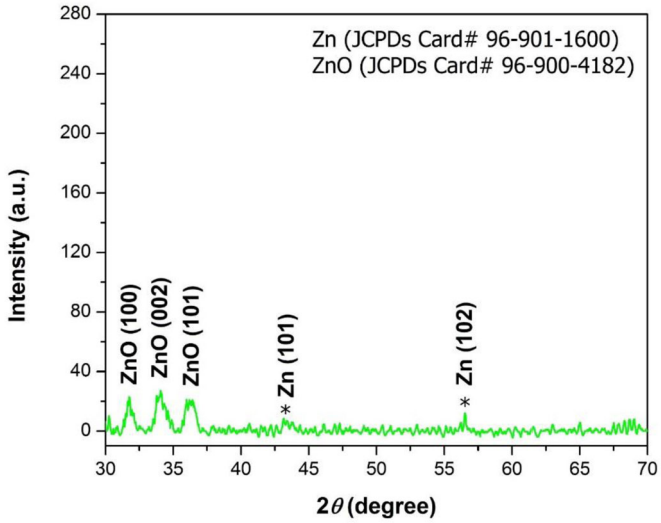

Figure 10. X-ray diffraction (XRD) analysis zinc oxide (ZnO) nanoparticles.

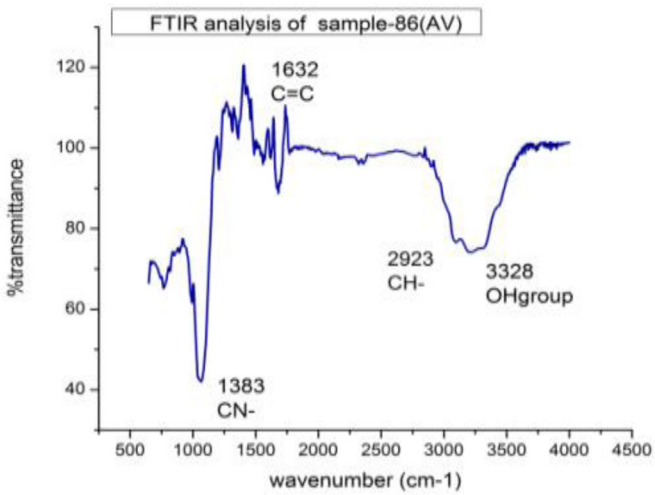

Figure 13. FTIR spectral analysis of iron oxide (Fe_2O_3) biogenically fabricated nanoparticles.

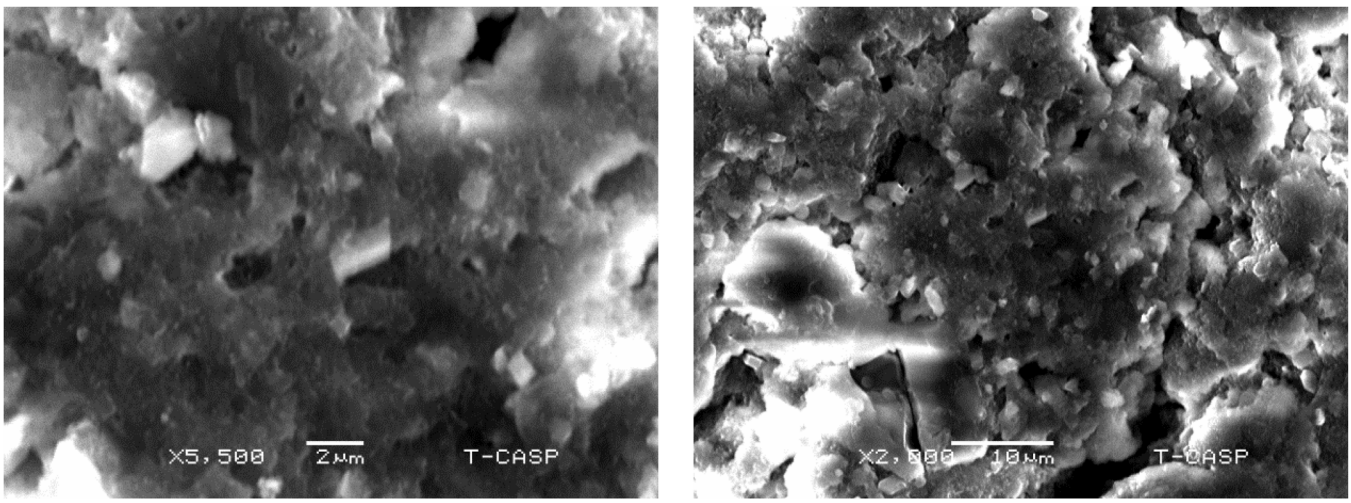

Figure 11. SEM analysis of iron oxide (Fe_2O_3) biogenically fabricated nanoparticles.

summarized in Table 4. Zinc oxides being least particles sized retained maximum ZOI against bacterial and fungal strains, but it was also demonstrated that antibacterial assay by TMO-NPs provided better results than antifungal activity. It was concluded that the antibacterial and antifungal activity of the MO-NPs elevated by increasing in surface/volume ratio and decreasing the particle sizes. Similarly, it was also to be noted that gram negative bacterial strains had the highest inhibition zone than gram-positive bacterial strains especially in the case of zinc oxides, copper oxide, and iron oxide nanomaterials. This could also be due to gram negative strains resistance.

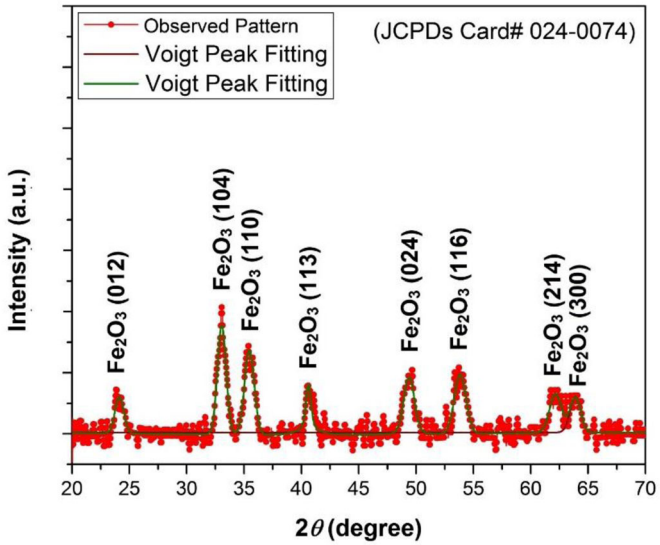

Figure 14. X-ray diffraction (XRD) analysis of iron oxide (Fe_2O_3) biogenically fabricated.

We reported in recent research that, smaller the particle size of MO-NPs, efficiency in ZOI against bacterial and fungal strains enhanced, assay efficiency depends on both the production of reactive oxygen species (ROS) and the accumulation of the nanoparticles too. A comparison of different nanomaterials from literature with a mechanism of action of antimicrobial activity were summarized in Table 2. It was observed with inhibition zones studies, zinc oxide nanoparticles had least efficiency against *A. niger* and *C. albicans* fungal strains. Thus, in this article, ZnO nanoparticles had shown the best antibacterial and antifungal activity. It was also assessed that the potential of antibacterial and antifungal activity is time-dependent, after 24 h the ZOI calculated found to be decreased due to bacterial growth (Results were summarized in Table 4). Minimum inhibitory concentration (MIC) values of zinc oxide nanoparticles for *E. coli, B. subtilis, B. licheniformis, K. pneumonia, A. niger, and C. albicans* were 01, 1.2, 1.2, 1.3, 1.7, and 02 while minimum bacterial concentration (MBA) values calculated were 0.8, 01, 01, 1.1, 1.2, and 1.4, respectively (Tables 4–6). It has resulted in TMO-NPs amount of 10 µg/mL had no harmful effect on human cells. Each assay was done in triplicate and the arithmetic mean, attributed to the corresponding results.

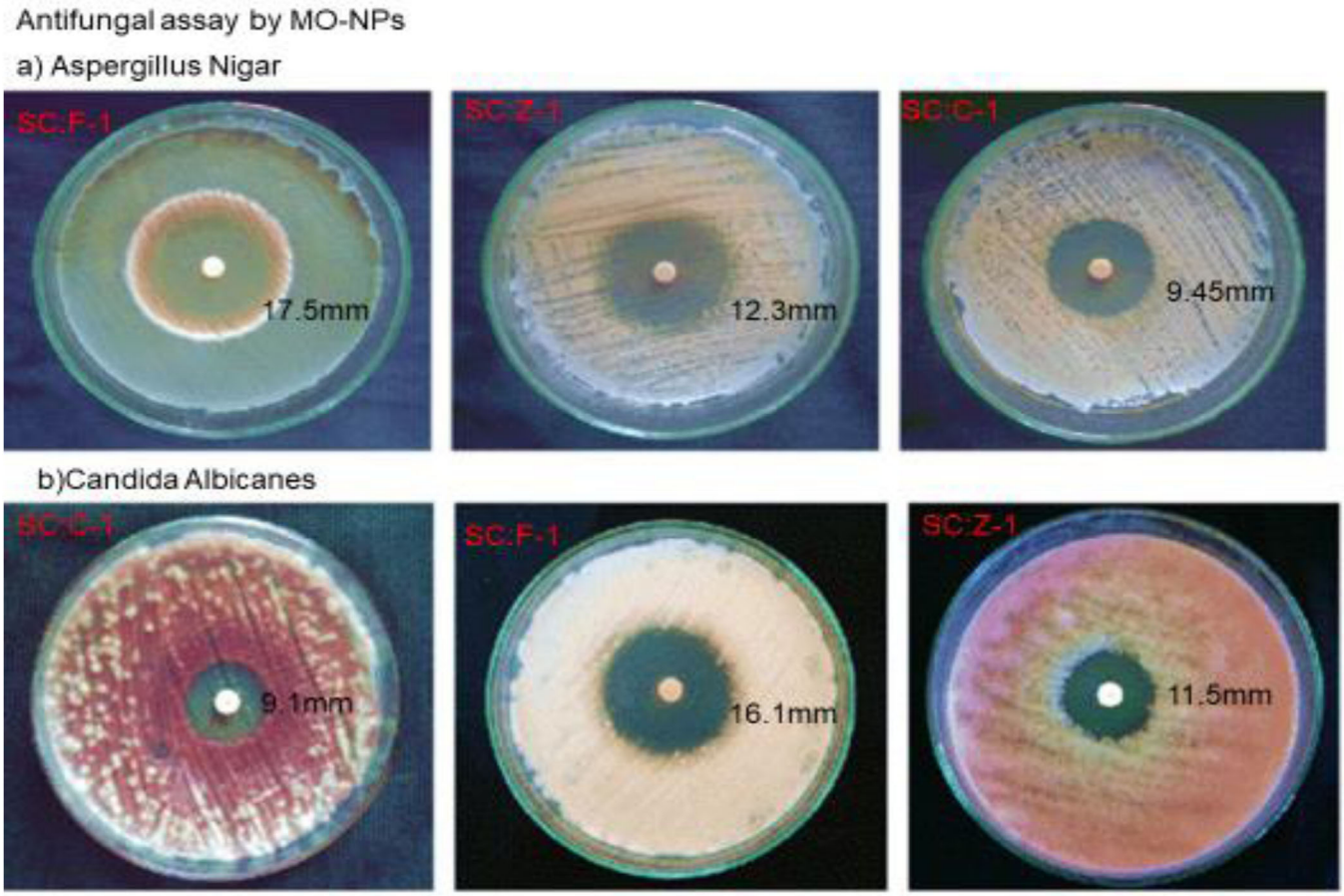

Figure 15. Antifungal analysis of sample code SC: Z-1, F-1 and C-1 against *Aspergillus niger* and *Candida albicans* fungal strain.

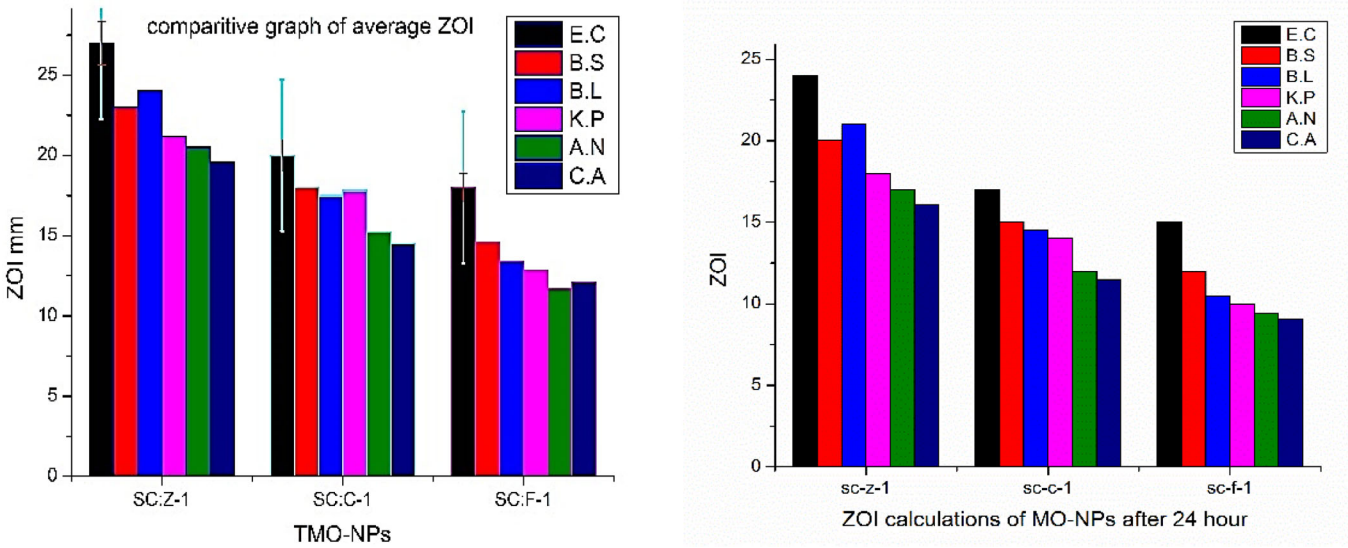

Figure 16. Comparative analysis of ZOI of TMO-NPs against bacterial and fungal strains before and after 24 h.

Comparative graphical estimation of ZOI of TMO-NPs against bacterial and fungal strains is summarized in Figure 16.

Conclusions

Among the biogenically fabricated transition metal-oxides, ZnO-NPs demonstrated the highest antimicrobial activity against six analyzed microbial strains at a concentration of 10 µg/mL. It was also concluded that in preparation method, 0.9% saline solution application promoted full growth of bacterial strain which helped in the precision of result calculations. Comparatively, transition metal nano oxides ZOI, MIC and also MBA values calculation confirmed zinc oxide nanometal effectiveness against bacterial and fungal strains. The broth medium needs 24 h to grow the bacteria, while in saline solution the bacteria colonies simply added and spread over the surface of nutrient agar in the Petri plates. Another prominent and unique benefit of using saline solution was that in the broth medium, there was a problem related to the overgrowth of bacteria which results in complexity in the experiment. While in the saline solution further growth of bacteria did not occur unless it was transferred on the nutrient agar medium. After the evaluation of results, it was obvious that the use of transition metals oxides would be productive and safer for oral use. In future, another comparison of antimicrobial activity may be promoted by nano metal oxides. Order of antimicrobial action on pathogenic microbes was in this order SC: Z-1 ≥ C-1 ≥ F-1. Industrially application of zinc oxides nanoparticles should be applied in oral medicines and oral pastes for reduction of bacterial growth.

Acknowledgements

The reported research was supported by the GCU Lahore, Department of Zoology for providing all fungi and bacterial strains for analysis and facility of the lab.

ORCID

Sabir Ali Siddique http://orcid.org/0000-0002-2665-3080

References

1. Shah, M.; Fawcett, D.; Sharma, S.; Tripathy, S. K.; Poinern, G. E. J. Green Synthesis of Metallic Nanoparticles via Biological Entities. *Materials (Basel)* **2015**, *8*, 7278–7308. DOI: 10.3390/ma8115377.
2. Azam, A.; Ahmed, A. S.; Oves, M.; Khan, M. S.; Habib, S. S.; Memic, A. Antimicrobial Activity of Metal Oxide Nanoparticles against Gram-Positive and Gram-Negative Bacteria: A Comparative Study. Int. J. Nanomed. **2012**, *7*, 6003–6009. DOI: 10.2147/IJN.S35347.
3. Komolafe, O. Antibiotic Resistance in Bacteria – An Emerging Public Health Problem. *Malawi Med. J.* **2004**, *15*, 63–67, DOI: 10.4314/mmj.v15i2.10780.
4. Azam, A.; Ahmed, A. S.; Oves, M.; Khan, M. S.; Memic, A. Size-Dependent Antimicrobial Properties of CuO Nanoparticles against Gram-Positive and -Negative Bacterial Strains. Int. J. Nanomed. **2012**, *7*, 3527–3535. DOI: 10.2147/IJN.S29020.
5. Rajendra, R.; Balakumar, C.; Ahammed, H.; Jayakumar, S.; Vaideki, K.; Rajesh, E. Use of Zinc Oxide Nano Particles for Production of Antimicrobial Textiles. *Int. J. Eng. Sci. Technol.* **2010**, *2*, 202–208. DOI: 10.4314/ijest.v2i1.59113.
6. Awwad, A. M.; Salem, N. M.; Aqarbeh, M. M.; Abdulaziz, F. M. Green Synthesis, Characterization of Silver Sulfide Nanoparticles and Antibacterial Activity Evaluation. *Chem. Int.* **2020**, *6*, 42–48. DOI: 10.5281/zenodo.3243157.
7. Akl, M.; Mostafa, M.; Abdel Hamid, A. I.; Hassanin, E. E.; Abdel-Raouf, M. Assessment of the Antimicrobial Activities of Trioctylphosphine Oxide Modified Silica Nanoparticles. *Egypt. J. Chem.* **2019**, *0*, 0–0. DOI: 10.21608/ejchem.2019.15032.1910.
8. Bharathi, D.; Ranjithkumar, R.; Chandarshekar, B.; Bhuvaneshwari, V. Preparation of Chitosan Coated Zinc Oxide Nanocomposite for Enhanced Antibacterial and Photocatalytic Activity: As a Bionanocomposite. *Int. J. Biol. Macromol.* **2019**, *129*, 989–996. DOI: 10.1016/j.ijbiomac.2019.02.061.
9. Roy, S.; Rhim, J. W. Agar-Based Antioxidant Composite Films Incorporated with Melanin Nanoparticles. *Food Hydrocoll.* **2019**, *94*, 391–398. DOI: 10.1016/j.foodhyd.2019.03.038.
10. Raghunath, A.; Perumal, E. Metal Oxide Nanoparticles as Antimicrobial Agents: A Promise for the Future. *Int. J. Antimicrob. Agents.* **2017**, *49*, 137–152. DOI: 10.1016/j.ijantimicag.2016.11.011.

11. Rubilar, O.; Rai, M.; Tortella, G.; Diez, M. C.; Seabra, A. B.; Durán, N. Biogenic Nanoparticles: Copper, Copper Oxides, Copper Sulphides, Complex Copper Nanostructures and Their Applications. *Biotechnol. Lett.* **2013**, *35*, 1365–1375. DOI: 10.1007/s10529-013-1239-x.
12. Ahmad, A.; Ullah, S.; Ahmad, W.; Yuan, Q.; Taj, R.; Khan, A. U.; A. U.; Rahman, Khan, U. A. Zinc Oxide- Selenium Heterojunction Composite: Synthesis, Characterization and Photo-Induced Antibacterial Activity under Visible Light Irradiation. *J. Photochem. Photobiol. B Biol.* **2020**, *203*, 111743, DOI: 10.1016/j.jphotobiol.2019.111743.
13. Babu, A. T.; Antony, R. Green Synthesis of Silver Doped Nano Metal Oxides of Zinc & Copper for Antibacterial Properties, Adsorption, Catalytic Hydrogenation & Photodegradation of Aromatics. *J. Environ. Chem. Eng.* **2019**, *7*, 102840, DOI: 10.1016/j.jece.2018.102840.
14. Feroze, N.; Arshad, B.; Younas, M.; Afridi, M. I.; Saqib, S.; Ayaz, A. Fungal Mediated Synthesis of Silver Nanoparticles and Evaluation of Antibacterial Activity. *Microsc. Res. Tech.* **2020**, *83*, 72–80. DOI: 10.1002/jemt.23390.
15. Muthukumar, H.; Mohammed, S. N.; Chandrasekaran, N. I.; Sekar, A. D.; Pugazhendhi, A.; Matheswaran, M. Effect of Iron Doped Zinc Oxide Nanoparticles Coating in the Anode on Current Generation in Microbial Electrochemical Cells. *Int. J. Hydrogen Energy* **2019**, *44*, 2407–2416. DOI: 10.1016/j.ijhydene.2018.06.046.
16. Rolim, W. R.; Pelegrino, M. T.; de Araújo Lima, B.; Ferraz, L. S.; Costa, F. N.; Bernardes, J. S.; Rodigues, T.; Brocchi, M.; Seabra, A. B. Green Tea Extract Mediated Biogenic Synthesis of Silver Nanoparticles: Characterization, Cytotoxicity Evaluation and Antibacterial Activity. *Appl Surf Sci* **2019**, *463*, 66–74. DOI: 10.1016/j.apsusc.2018.08.203.
17. Ghosh, M.; Mandal, S.; Roy, A.; Chakrabarty, S.; Chakrabarti, G.; Pradhan, S. K. Enhanced Antifungal Activity of Fluconazole Conjugated with Cu-Ag-ZnO Nanocomposite. *Mater. Sci. Eng. C* **2020**, *106*, 110160, DOI: 10.1016/j.msec.2019.110160.
18. Kumar, L. V.; Nath, G. R. Synthesis, Characterization and Biological Studies of Cobalt(II), Nickel(II), Copper(II) and Zinc(II) Complexes of Vanillin-4-Methyl-4-Phenyl-3-Thiosemicarbazone. J. Chem. Sci. **2019**, *131*, 76, DOI: 10.1007/s12039-019-1658-x.
19. Bandeira, M.; Giovanela, M.; Roesch-Ely, M.; Devine, D. M.; da Silva Crespo, J. Green Synthesis of Zinc Oxide Nanoparticles: A Review of the Synthesis Methodology and Mechanism of Formation. *Sustain. Chem. Pharm.* **2020**, *15*, 100223. DOI: 10.1016/j.scp.2020.100223.
20. Pervaiz, M.; Ahmad, I.; Yousaf, M.; Kirn, S.; Munawar, A.; Saeed, Z.; Adnan, A.; Gulzar, T.; Kamal, T.; Ahmad, A.; Rashid, A. Synthesis, Spectral and Antimicrobial Studies of Amino Acid Derivative Schiff Base Metal (Co, Mn, Cu, and Cd) Complexes. *Spectrochim. Acta A Mol. Biomol. Spectrosc.* **2019**, *206*, 642–649. DOI: 10.1016/j.saa.2018.05.057.
21. Henam, S. D.; Ahmad, F.; Shah, M. A.; Parveen, S.; Wani, A. H. Microwave Synthesis of Nanoparticles and Their Antifungal Activities. *Spectrochim. Acta A Mol. Biomol. Spectrosc.* **2019**, *213*, 337–341. DOI: 10.1016/j.saa.2019.01.071.
22. Espitia, P. J. P.; Soares, N.; de, F. F.; Coimbra, J. d R.; de Andrade, N. J.; Cruz, R. S.; Medeiros, E. A. A. Zinc Oxide Nanoparticles: Synthesis, Antimicrobial Activity and Food Packaging Applications. *Food Bioprocess Technol.* **2012**, *5*, 1447–1464. DOI: 10.1007/s11947-012-0797-6.
23. Leonard, H.; Colodner, R.; Halachmi, S.; Segal, E. Recent Advances in the Race to Design a Rapid Diagnostic Test for Antimicrobial Resistance. *ACS Sens.* **2018**, *3*, 2202–2217. DOI: 10.1021/acssensors.8b00900.
24. Saqib, S.; Zaman, W.; Ullah, F.; Majeed, I.; Ayaz, A.; Hussain Munis, M. F. Organometallic Assembling of Chitosan-Iron Oxide Nanoparticles with Their Antifungal Evaluation against *Rhizopus oryzae*. *Appl. Organomet. Chem.* **2019**, *33*, e5190, DOI: 10.1002/aoc.5190.
25. Devi, H. S.; Boda, M. A.; Shah, M. A.; Parveen, S.; Wani, A. H. Green Synthesis of Iron Oxide Nanoparticles Using *Platanus orientalis* Leaf Extract for Antifungal Activity. *Green Process Synth.* **2019**, *8*, 38–45. DOI: 10.1515/gps-2017-0145.